Systematic position of *Discocephalus*-like ciliates (Ciliophora: Spirotrichea) inferred from SSU rDNA and ontogenetic information

Chen Shao,[1] Weibo Song,[1,2] Lifang Li,[1] Alan Warren,[3]
Khaled A. S. Al-Rasheid,[4] Saleh A. Al-Quraishy,[4] Saleh A. Al-Farraj[4]
and Xiaofeng Lin[2]

Correspondence
Weibo Song
wsong@ouc.edu.cn

[1]Laboratory of Protozoology, Ocean University of China, Qingdao 266003, PR China

[2]Laboratory of Protozoology, College of Life Science, South China Normal University, Guangzhou 510631, PR China

[3]Department of Zoology, Natural History Museum, Cromwell Road, London SW7 5BD, UK

[4]Zoology Department, King Saud University, PO Box 2455, Riyadh 11451, Saudi Arabia

The *Prodiscocephalus*-like ciliates, or discocephalines, are cephalized organisms that are traditionally considered to be hypotrichs (*sensu lato*) but whose precise systematic position has long been uncertain. The main reasons for this are that these organisms exhibit several intermediate morphological and morphogenetic features and that hitherto none has been investigated using molecular methods. In the present study, the cortical development of *Prodiscocephalus borrori* was observed during binary division and this can be summarized as follows: (i) in the parental adoral zone of membranelles, only the posterior end is renewed by dedifferentiation of the old structures; (ii) the oral primordium in the opisthe occurs *de novo* on the cell surface as seen in other typical stichotrichs; (iii) in both dividers, the undulating membranes anlage does not split longitudinally in the usual way but, instead, divides transversely to form the paroral and endoral membranes; (iv) usually seven frontoventral transverse cirral anlagen are formed in the primary mode which then divide into two sets, one each for the proter and opisthe; (v) both left and right marginal rows divide into two parts, thus giving rise to a post-lateral marginal segment at the posterior end of each; (vi) invariably five caudal cirri are formed at the posterior end of the three rightmost dorsal kinety anlagen. Thus, it was found that, like other related discocephalines, *P. borrori* exhibits more similarities to stichotrichs than to euplotids. Based on a combination of morphological and morphogenetic data, a phylogenetic tree was constructed which suggests that the discocephalines group within the stichotrichs and separate from the euplotids. In addition, the complete small-subunit rRNA gene (SSU rDNA) of *P. borrori* was sequenced and analysed. In the resulting SSU rDNA tree, the discocephalines represent an intermediate group between the euplotids and the Stichotrichia–Oligotrichia–Choreotrichia assemblage, albeit with low bootstrap support. From these data, we conclude that the discocephalines might be a divergent, or possibly an ancestral, group within the Stichotrichia. Furthermore, our findings further support the suggestion that these organisms should be considered as a distinct order, i.e. Discocephalida Wicklow, 1982, in the subclass Stichotrichia Small & Lynn, 1985.

INTRODUCTION

The discocephaline ciliates, which are characterized by their cephalized body shape, psammophilic habitat and unique combination of morphological features, are one of the most confused groups within the traditional 'hypotrichs' *sensu lato* (*s. l.*) (i.e. including both stichotrichs and euplotids) regarding their phylogenetic relationships. Corliss (1979) regarded the discocephalines as a genus-complex which he tentatively placed in the family Euplotidae, order

Hypotrichida. Jankowski (1979), however, treated them as a family within the order Sporadotrichina. Subsequently, Wicklow (1982) upgraded them to suborder within the order Hypotrichida (*s. l.*), whereas Small & Lynn (1985) classified them as a suborder in the Euplotida. Tuffrau (1986) assigned them to Hypotrichida (*s. l.*) and as a suborder along with Euplotina, Stichotrichina and Sporadotrichina. de Puytorac *et al.* (1993) established the order Discocephalida within the subclass Oxytrichia (class Hypotrichea), which was subsequently accepted by Tuffrau & Fleury (1994). More recently, Lynn & Small (2000) retained the arrangement they suggested previously (Small & Lynn, 1985), with Discocephalina as a sister group to Euplotina in the order Euplotida.

There are a number of reasons for this confusion: (i) patterns of morphogenesis within this group are poorly understood, with only two discocephaline taxa, *Marginotricha* and *Discocephalus*, having been studied morphogenetically; (ii) there is a complete absence of molecular data; (iii) many morphological and morphogenetic features present in discocephalines are shared by different ranks of hypotrichs and/or stichotrichs (Wicklow, 1982; Foissner, 1996; Lin *et al.*, 2004).

In the spring of 2005, a population of *Prodiscocephalus borrori* (Wicklow, 1982) was isolated from marine sediments near Qingdao, China, enabling studies of its morphogenesis to be carried out, its small-subunit rRNA gene (SSU rDNA) to be sequenced and its phylogenetic position to be analysed. The aims of the present paper are (i) to increase our knowledge and understanding of morphogenesis in discocephalines and (ii) to re-evaluate the systematic position of the discocephalines based on morphological, morphogenetic and molecular data.

METHODS

Morphological and morphogenetic studies. Samples were collected on 8 May 2005 from the surface of sandy littoral sediments (up to 5 cm deep) in Jiaozhou Bay near Qingdao, China (120° 18′ E 36° 04′ N). Isolated specimens were maintained in the laboratory for about 1 week as uniprotistan cultures (water temperature about 20 °C, salinity ~30‰) in Petri dishes for observation and further studies. Cells in division were selected and then impregnated using the protargol method (Wilbert, 1975). Drawings were made using a camera lucida at ×1250 magnification. To illustrate the changes during morphogenetic processes, parental cirri are depicted in outline, whereas new ones are shaded black. Terminology and systematics are mainly according to Wicklow (1982) and Lynn & Small (2000).

SSU rDNA sequence and phylogenetic analyses. Genomic DNA extraction, PCR amplification of the SSU rDNA, cloning and sequencing were performed according to Li & Song (2006). The nucleotide sequences used in this study are available from the GenBank/EMBL/DDBJ databases, including 21 species sequenced by the senior author's laboratory (see Supplementary Table S1, available in IJSEM Online).

Sequences were aligned using CLUSTAL W v. 1.80 (Thompson *et al.*, 1994) and then the alignment was refined through consideration of

conserved secondary structures. A 50 % majority-rule Bayesian inference (BI) tree was constructed with MrBayes 3.1.2 (Ronquist & Huelsenbeck, 2003) using the GTR+G+I evolutionary model indicated by Mrmodeltest v.2 (Nylander, 2004). The chain length for our analysis was 10 000 000 generations, with trees sampled every 100 generations. The first 2 500 000 generations were discarded as burn-in.

A maximum-likelihood (ML) tree was constructed with PAUP (v. 4.0b10) (Swofford, 2002) using the TrN+I+G evolutionary model selected by Modeltest (Posada & Crandall, 1998) and an input file created by performing an accelerated likelihood surface exploration (Nixon, 1999; Vos, 2003) with the program PAUPRat (Sikes & Lewis, 2001). A 50 % majority-rule consensus ML tree was derived from the output of 200 trees generated by PAUP operating on the input file from PAUPRat.

The topologies of the BI and ML trees were almost identical. Therefore, they were merged into a single tree for purposes of illustration. This tree was formatted with MEGA (Kumar *et al.*, 2004) and exported from it as a graphics file for construction of the finished figure.
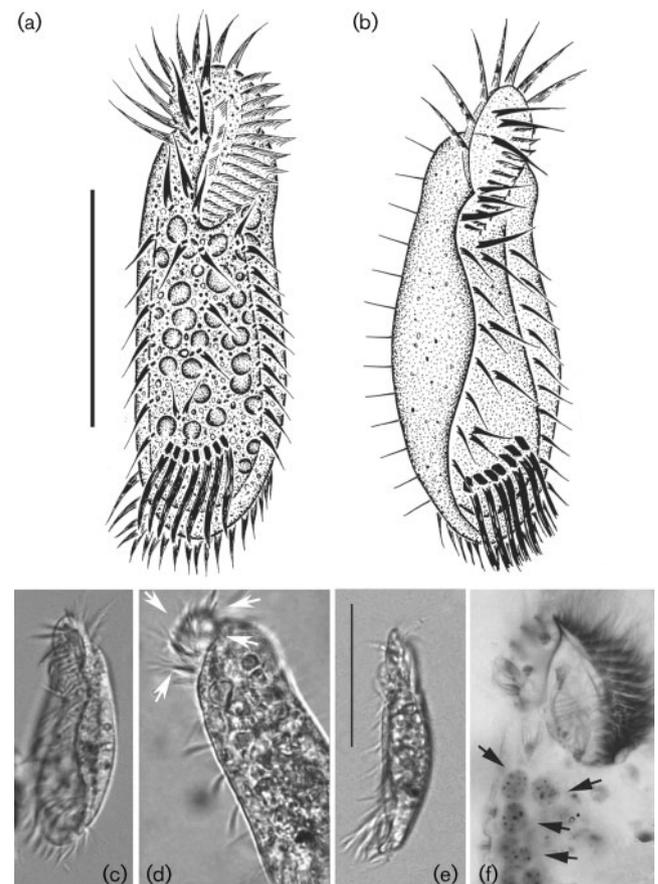

Fig. 1. *P. borrori in vivo* (a–e) and after protargol impregnation (f) (after Lin *et al.* 2004, with permission). (a) Ventral view of a typical individual. (b, c) Ventral-lateral views. (d) Dorsal view, to show the discoid 'head' (arrows). (e) Lateral view. (f) Anterior portion, to show macronuclear nodules (arrows). Bars, 40 μm (a; also applies to b) and 50 μm (e; also applies to c, d, f).

RESULTS

Morphology of *Prodiscocephalus borrori* (Wicklow, 1982) Lin *et al.*, 2004 (Figs 1 and 2a–c)

The population of *P. borrori* studied here corresponds very closely with the population reported by Lin *et al.* (2004), hence a detailed description is unnecessary. As Figs 1 and 2(a–c) demonstrate, this species has a slender body shape, prominent transverse cirri, invariably 12 frontoventral cirri that are sparsely distributed and one marginal row on each side. It should also be noted that two short fragments with close-set cirri (post-lateral left and right marginal cirri; PLMC, PRMC in Fig. 2b) are located posterior to the left and right marginal rows, respectively, and that the five caudal cirri are arranged in three rows with the pattern of 1:2:2 from left to right (arrows in Fig. 2b). By contrast, Lin *et al.* (2004) reported that the number of caudal cirri is variable, but this was almost certainly due to confusion with the post-lateral right marginal cirri (PRMC in Fig. 2b)
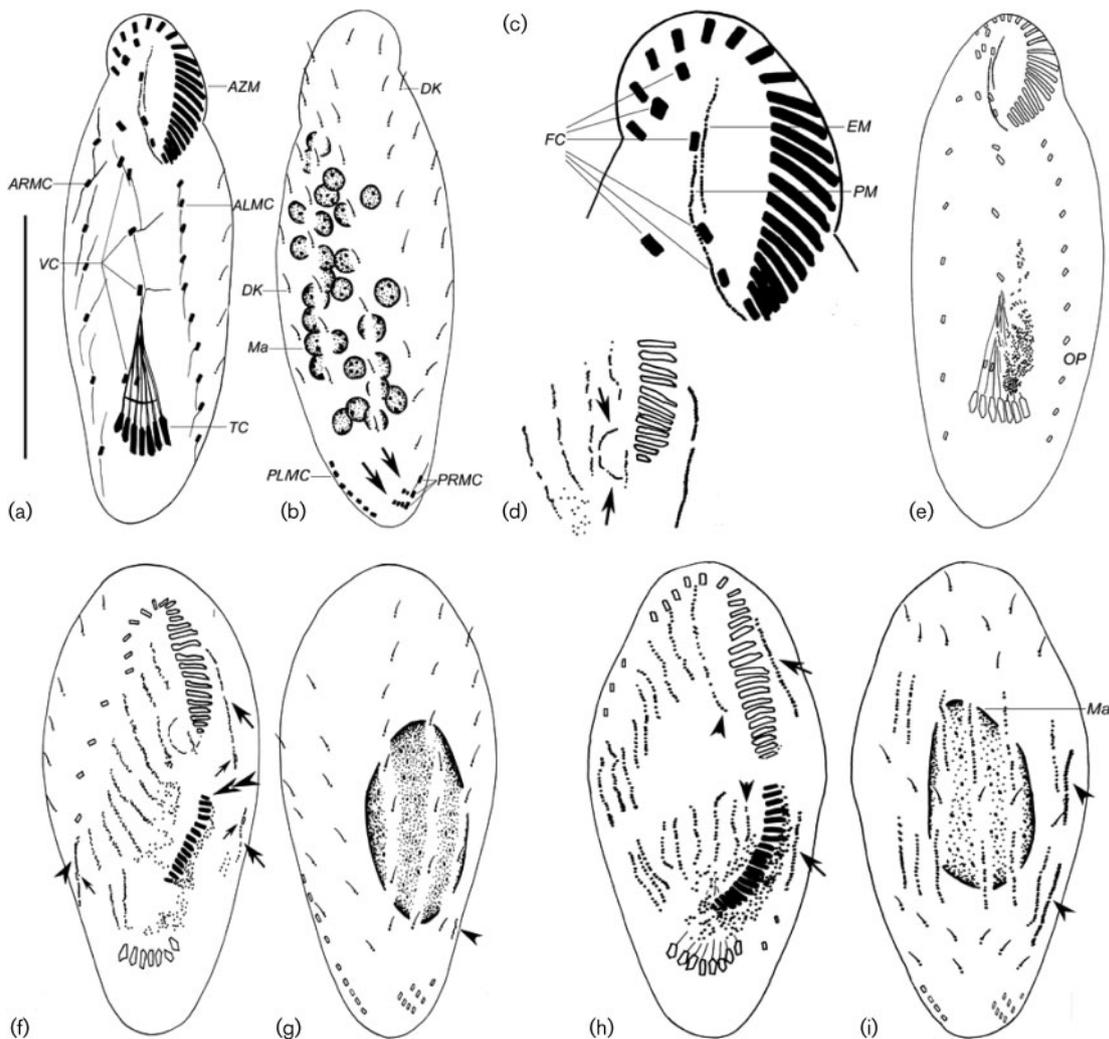
Fig. 2. *P. borrori* before division (a–c) and in the early stages of morphogenesis (d–i) after protargol impregnation. (a, b) Ventral and dorsal views of the same specimen, to demonstrate the general pattern of the infraciliature. Arrows in (b) mark the caudal rows. (c) Infraciliature of the anterior portion of the cell. (d) Detail of ventral view in an early divider, to show the curved structure (UM-anlage; arrows). (e) Ventral view of a divider in very early stage. (f, g) Ventral and dorsal views of the same specimen, to show the right (arrowheads) and left (large arrows) marginal anlagen; the double arrowhead marks the newly formed OP and small arrows show the old marginal cirri. (h, i) Slightly later stage, ventral and dorsal views of the same cell; note that the FVT- and DK anlagen are completely formed in both dividers. Arrows in (h) show the left marginal row anlagen, arrowheads mark the UM-anlage; arrowheads in (i) depict the right marginal row anlagen. ALMC, Anterior left marginal cirri; ARMC, anterior right marginal cirri; AZM, adoral zone of membranelles; DK, dorsal kinety; EM, endoral membrane; FC, frontal cirri; Ma, macronuclear nodule; OP, oral primordium; PLMC/PRMC, post-lateral left/right marginal cirri; PM, paroral membrane; TC, transverse cirri; VC, ventral cirri. Bar, 40 μm.

being erroneously counted as caudal cirri. These two types of cirri can be recognized clearly during morphogenesis but are almost impossible to distinguish in non-dividing cells.

## Morphogenesis of the Qingdao population of *P. borrori* during binary fission (Figs 2d–i, 3, 4 and 5)

Oral primordia (OP). *P. borrori* demonstrates an epi-apokinetal pattern of morphogenesis with respect to the formation of the OP in the opisthe and a mixture of typical stichotrich and euplotid modes regarding the development of the somatic ciliature. The main processes are as follows. The OP appears on the cell surface below the equatorial level (Fig. 2e). Soon after, the membranelles are generated, beginning at the anterior end of the OP posteriad, and these will form the adoral zone of membranelles (AZM) of

the opisthe (Fig. 2f, double arrowheads; Fig. 4d, arrow). In the early stage, the anterior portion of the old undulating membranes (UM) appears to be resorbed, whereas the posterior part appears to dedifferentiate and develops into a curved structure that will be the anlage for the UM (arrows in Figs 2d and 4c). Later, the leftmost frontal cirrus is formed and separates from the UM anlage in both dividers (Fig. 3a, arrows; Fig. 4f, i, arrow). When most of the new membranelles are formed in the OP, the proximal end of the parental AZM begins to disorganize (Fig. 3a, arrowhead).

The endoral and paroral membranes, which are derived from the UM-anlage by segmentation, are initially confluent but then separate from each other as the latter arches to the left (Fig. 3 g, arrows and double arrowheads; Fig. 5g, h, arrow).
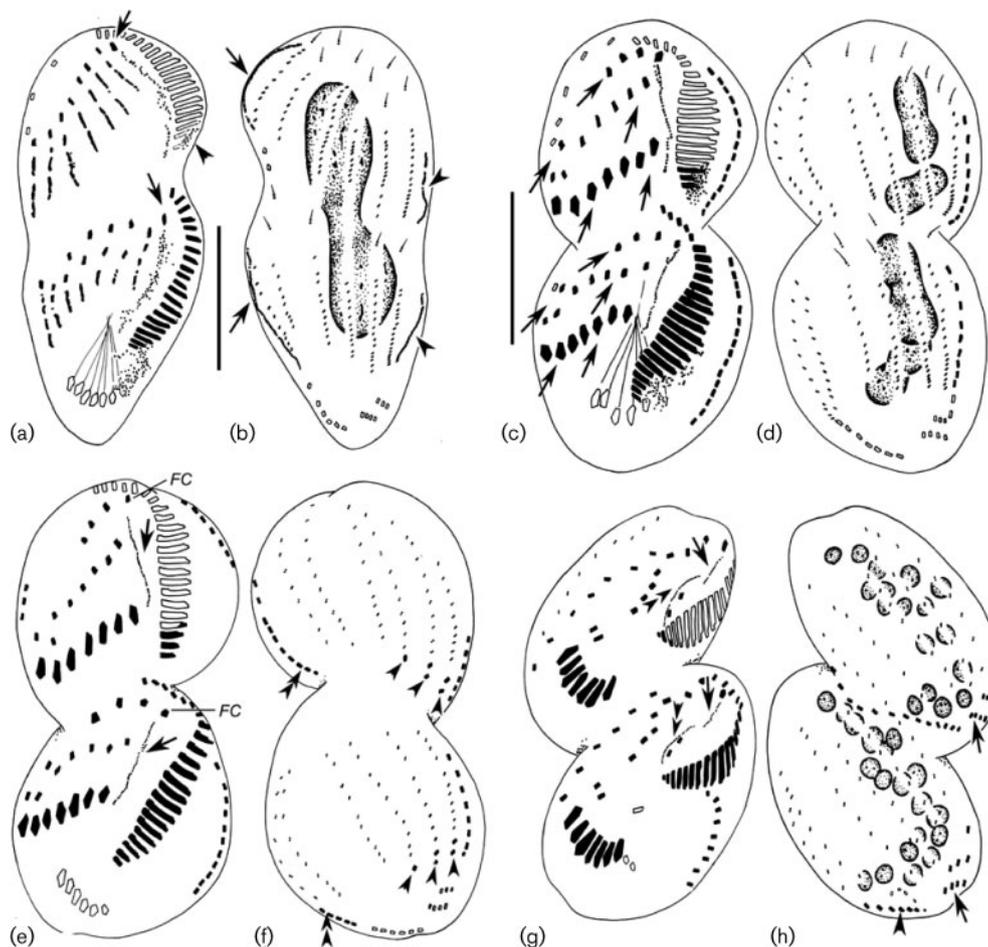
Fig. 3. Middle and late morphogenetic stages in *P. borrori*. (a) Ventral view, to show the UM-anlage generating the anteriormost FC in both dividers (arrows) and the FVT-anlagen beginning to segment. Note the proximal end of the old AZM beginning to dedifferentiate (arrowhead). (b) Dorsal view of the same cell as in (a), to show the left (arrows) and right (arrowheads) marginal row anlagen. (c, d) Ventral and dorsal views of the same specimen, showing the FVT cirri (arrows in c). (e, f) Ventral and dorsal views of the same cell; note the UM-anlage is still single-rowed (arrows), and the caudal cirri are differentiated from DK anlagen (arrowheads). Double arrowheads in (f) mark the post-lateral marginal cirri. (g) Ventral view, showing the separated paroral (double arrowheads) and endoral (arrows) membranes. (h) Dorsal view of the same specimen as in (g); arrows mark five caudal cirri, arrowhead shows the post-lateral marginal cirri. FC, Frontal cirri. Bars, 40 μm.
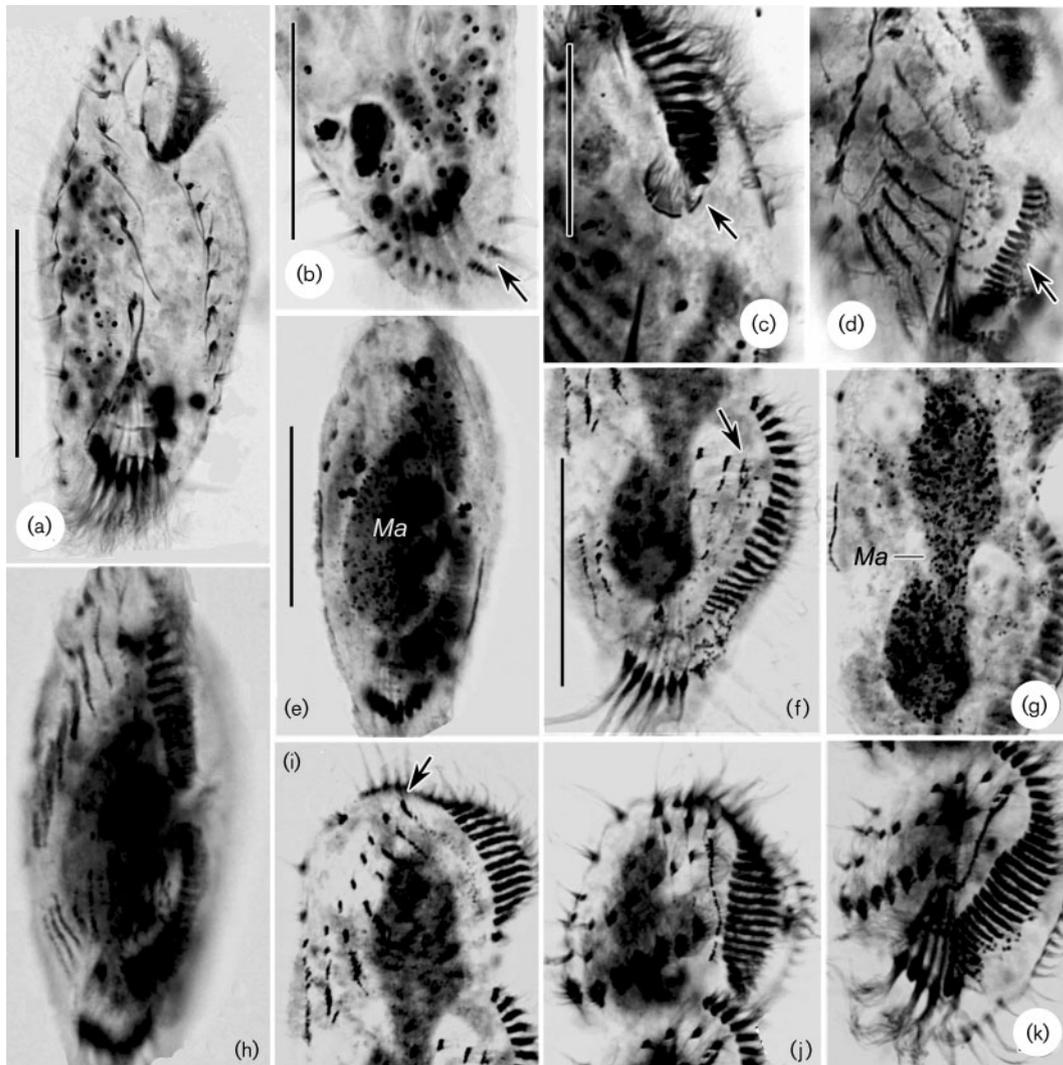
Fig. 4. Photomicrographs of the morphology (a, b) and morphogenesis (c–k) of *P. borrori* after protargol impregnation. (a) Ventral view of a non-dividing cell. (b) Detail of the posterior portion of the cell. Note the caudal cirri (arrow). (c) Ventral view of the proter in an early division stage, to demonstrate the curved UM-anlage (arrow). (d) Ventral view, showing the new membranelles formed in the OP (arrow). (e) Showing the fusion of the macronuclear nodules into a single mass (Ma). (f) Ventral view of a mid-stage divider, to show the UM-anlage generating the anteriormost frontal cirrus in the opisthe (arrow). (g) The macronucleus (Ma) in division. (h) Ventral view of an early divider, showing the streaks of the FVT-anlagen. (i) Ventral view; note the anteriormost frontal cirrus developing from the UM-anlage in the proter (arrow). (j, k) Showing the segmentation of the FVT-anlagen in both proter (j) and opisthe (k). Bars, 40 µm (a, b, e, f) and 20 µm (c; also applies to d). Note that (g–k) are the same magnification as (f).

Cirral streaks. Seven or eight frontoventral transverse (FVT) anlagen are generated to the right of the parental oral apparatus as oblique streaks, the old structures apparently not being involved in the formation of these new anlagen (Figs 2f and 4d). These streaks appear initially as a single set (primary pattern) that subsequently divides into two groups (Fig. 2h). Finally, the FVT-anlagen are segregated in the pattern of 3:3:3:2:2:3:2 from left to right (Fig. 3a, c, showing the specimens with only seven cirral primordia). Thus, with the frontal cirrus from the anterior end of the UM

anlage, a total of 19 FVT-cirri are formed. It is therefore assumed that, in those cells with eight FVT-anlagen, the extra cirri produced by the additional anlage are resorbed prior to the completion of the division process.

Marginal and dorsal kineties (DK) anlagen. The new marginal rows are generated intrakinetally in the usual manner for stichotrichs (Figs 2f–i and 3). Nevertheless, at the very late stage, about four to eight cirri in the posterior portion of the left marginal row and three or four cirri in
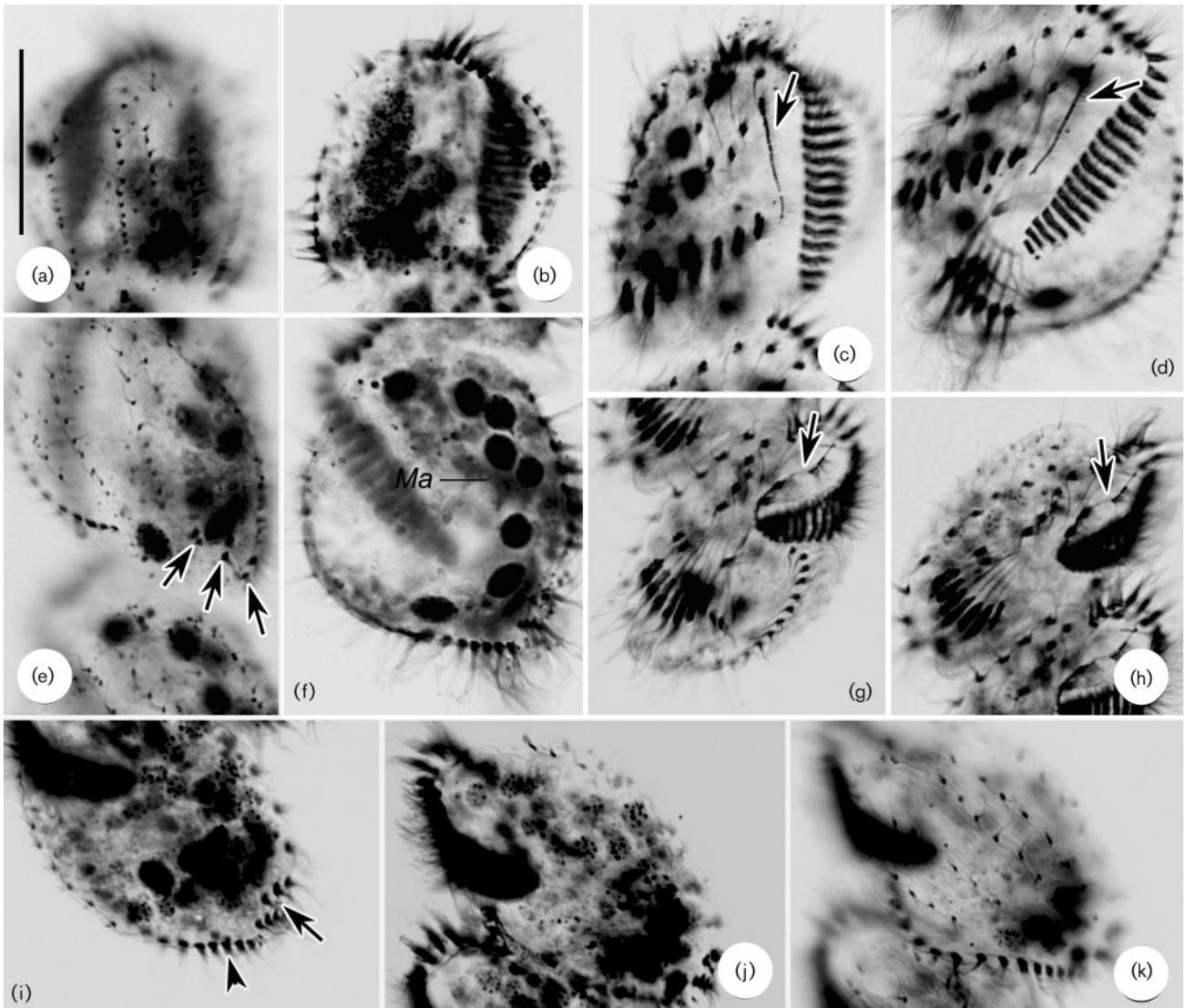
Fig. 5. Photomicrographs of *P. borrori* during morphogenesis. (a, b) Dorsal and ventral views; note that the DK anlagen stretch to both ends of the cell. (c–e) Ventral (c, d) and dorsal (e) views of the same divider. Note the single-rowed UM-anlage in both proter (arrow in c) and opisthe (arrow in d). Arrows in (e) showing five caudal cirri differentiated from DK4 (1), DK5 (2) and DK6 (2), respectively. (f) Macronuclear nodules (Ma) in division having previously been fused into a single mass. (g, h) Ventral views of the same cell. Note that the endoral and paroral membranes develop from the UM-anlage in the opisthe (arrow in g) and proter (arrow in h). (i–k) Dorsal views of a divider just before separation (focusing on different levels). The arrow in (i) points to the caudal cirri; arrowhead shows the left post-lateral marginal cirri. Note the macronuclear nodules (j) and dorsal kineties (k). Bar, 40 μm.

the posterior portion of the right marginal row migrate to the dorso-marginal side, giving rise to the post-lateral left and right marginal fragments, respectively (Fig. 3f, double arrowheads; Figs 3h and 5i, arrowhead).

The formation of dorsal kineties exhibits a urostylid (i.e. secondary) mode in that the two sets of DK anlagen are generated intra-kinetally within the old rows in both dividers (Figs 2i and 3b, d). In contrast, the five caudal cirri are generated in a euplotid mode, i.e. the three rows are formed at the posterior ends of the three rightmost dorsal

kineties in the pattern of 1 : 2 : 2 (Fig. 3f, arrowheads; Figs 3h and 5e, arrows; Fig. 5i, arrow).

All macronuclear nodules (Ma) fuse into a single mass prior to division in the usual way.

SSU rDNA sequence analysis

The SSU rDNA of *P. borrori* was newly sequenced (length 1769 nucleotides). Alignment of this sequence clearly showed similarities in primary structure and G + C
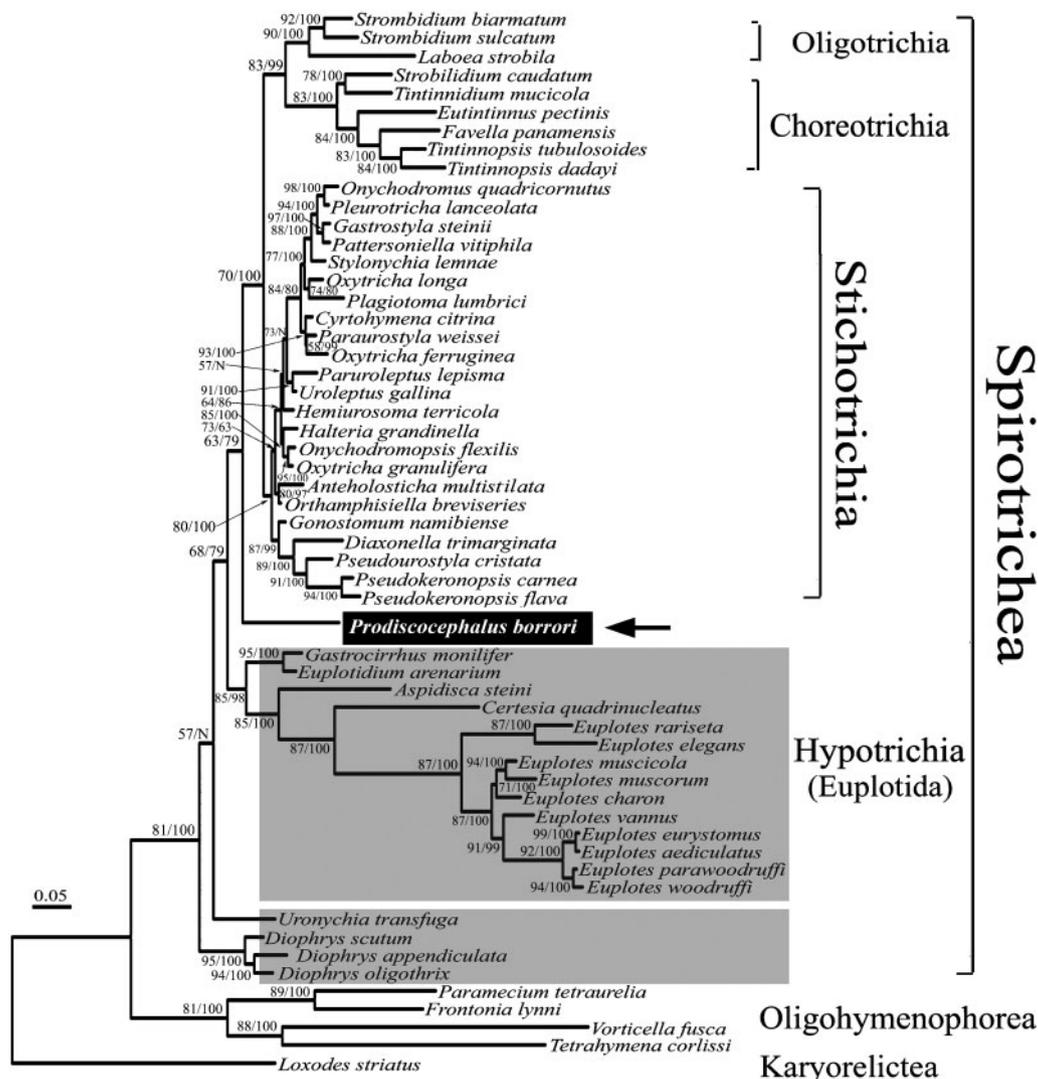
Fig. 6. Bayesian tree inferred from nucleotide sequences of the SSU rDNA. Numbers at nodes represent bootstrap values (%) from 1000 replicates: the first number is the Bayesian credibility value using the MrBayes algorithm and the second is from the ML method; N, not significant. *Loxodes striatus* was selected as the outgroup taxon. Evolutionary distance is represented by the branch length to separate the species in the figure. Bar, 5 substitutions per 100 nucleotide positions.

content (44.6 mol%) to other spirotrichous ciliates (Sogin & Elwood, 1986; Schlegel *et al.*, 1991). The structural similarities were 78.07–88.83 % between *P. borrori* and euplotids and 86.05–89.91 % compared with stichotrichs.

Bayesian analyses based on the sequence of the SSU rDNA. The phylogenetic trees constructed using different methods gave identical topological structure, hence only one tree is presented here (Fig. 6). The analyses provide moderate to high bootstrap support for the monophyly of Stichotrichia (80 % BI, 100 % ML) and most of Hypotrichia (85 % BI, 98 % ML), i.e. all typical euplotids except the *Diophrys–Uronychia* assemblage, which branches from the spirotrichous clade at a deep level though with low bootstrap support. The monophyly of each of the other

two spirotrich subclasses, Choreotrichia (83 % BI, 100 % ML) and Oligotrichia (90 % BI, 100 % ML), is also confirmed, as expected. *P. borrori* is placed between the Stichotrichia–Choreotrichia–Oligotrichia clade and the Hypotrichia clade and is sister to the former.

DISCUSSION

Traditionally, the discocephalines have been separated from the stichotrichs and the euplotids by their cephalized body shape, highly differentiated infraciliature (which is similar to that of oxytrichids) and extremely well-developed fibre system and by being invariably psammophilic (Dragesco, 1960, 1965; Wicklow, 1982; Curds & Wu, 1983; Lin *et al.*, 2004). There is little agreement, however,

Table 1. Comparison of morphogenetic characteristics among three higher hypotrichous groups

The higher stichotrichs represent the genera in the oxytrichid complex (*s. l.*), whereas the lower stichotrichs are the typical urostylids. Data for the euplotids are from genera for which morphogenesis is well characterized (e.g. *Euplotes*, *Diophrys*, *Uronychia* and *Aspidisca*, respectively abbreviated as *Eup.*, *Dio.*, *Uro.* and *Asp.*).

Character	Higher stichotrichs	Lower stichotrichs	Euplotids	*Discocephalus ehrenbergi*	*Marginotricha faurei*	*Prodiscocephalus borrori*
Fate of old AZM	Completely retained	Mostly renewed	Retained (*Eup.* and *Asp.*) or partly renewed (*Dio.*)	Completely retained	Partly renewed	Partly renewed
Fate of old UM	Completely renewed	Completely renewed	Retained (*Eup.* and *Asp.*) or completely renewed (*Dio.*)	Completely renewed	Completely renewed	Completely renewed
Origin of the opisthe's OP	On cell surface	On cell surface	Within a subsurface pouch, beneath the pellicle	On cell surface	On cell surface	On cell surface
FVT-cirral anlagen, number	5 FVT-anlagen	More than 5	5 FVT-anlagen	More than 5	More than 5	More than 5
Type of development of FVT-anlagen	Almost absolutely secondary	Mostly secondary, less commonly primary	Primary formation	Primary formation	Primary formation	Primary formation
Marginal anlagen	Intrakinetally	Intrakinetally	*De novo*	Intrakinetally	Intrakinetally	Intrakinetally
DK anlagen type*	Mostly two-group type; less commonly one group	One-group type	One-group type	One-group type	One-group type	One-group type
DK formation mode†	Secondary	Secondary	Primary	Secondary	Secondary	Secondary
Origin and process of DK	Within left parental rows, followed by fragmentation	Within each of parental one	Within each of parental one, no fragmentation	As in lower stichotrichs, no fragmentation	As in lower stichotrichs	As in lower stichotrichs
Formation of caudal cirri‡	One	One (mostly); two (in few genera)	Two (*Dio.*, *Uro.*); one (*Eup.*)	Two	Two	Two
Sources of data	Berger (1999); Song (2004)	Berger (2006); Song (2004)	Song & Packroff (1993); Song (2004); Song *et al.* (2004)	Wicklow (1982)	Wicklow (1982)	Present work

*One group generates intrakinetally from the parental DK, the other is formed *de novo* dorsal-marginally.
†Initially as one group and then divides into two sets, one for each divider (primary mode) or initially as two groups for two daughter cells (secondary mode).
‡Indicated as one [when present, the DK anlagen (usually the left ones) generate only one caudal cirrus each] or two (when present, two or more caudal cirri may be differentiated from the rightmost DK anlage).
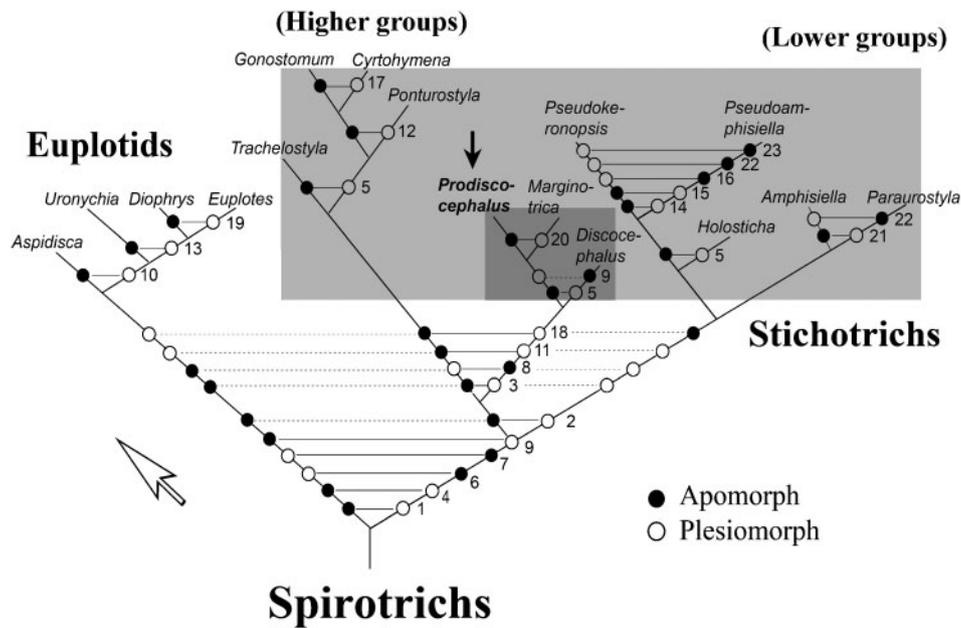
Fig. 7. Assessment of the phylogenetic position of *P. borrori* and some other representative stichotrichs–euplotids based on morphological and morphogenetic information. The light shaded area shows the stichotrichs and the dark shaded area shows the discocephalines. The arrow indicates the tentative evolutionary direction. See Table 2 for an explanation of the characters used.

Table 2. Morphogenetic and morphological characters on which the phylogenetic tree for representatives of discocephalines and other spirotrichous genera is based (Fig. 7)

Data were taken from Wicklow (1982), Song (1990, 2001), Jerka-Dziadosz & Wiernicka (1992), Song & Packroff (1993), Eigner & Foissner (1994), Song *et al.* (1997, 2004), Berger (1999, 2006), Hu & Song (2001) and Shao *et al.* (2006, 2007).

Character	Apomorph	Plesiomorph
1	Formation of OP in opisthe in subapokinetal mode	In epi-apokinetal mode
2	Number of cirral streaks stable	Variable in number
3	Five-TC, five-cirrus-anlagen mode	Not five-TC, non-five-cirrus-anlagen mode
4	UM in proter forms *de novo* from isolated anlage structure	Rebuilt within the old structure
5	New OP formed in the proter	No new OP formed in the proter
6	DK formed in secondary mode	In primary mode
7	Cirri organized in groups or in patterns	Not in groups nor (generally) in patterns
8	Formation of caudal cirri in euplotid mode	Not in euplotid mode
9	Right marginal row absent	Present
10	Left marginal row absent	Present
11	DK not formed in each old row, often grouped	Intrakinetally in each old row
12	One marginal row on each side	More than one on each side
13	AZM in two parts	AZM in one part
14	Frontoterminal cirri present	Absent
15	Macronuclear nodules do not fuse into a single mass	Fusion into a single mass
16	Midventral rows in typical zig-zag pattern	Two rows widely separated
17	Cell with a distinctive 'head' or cephalized	Not cephalized
18	FVT-cirral anlagen formed in secondary mode	In primary mode
19	Two undulating membranelles	Single undulating membrane
20	Ventral cirri sparsely distributed	Densely packed or aligned in a row(s)
21	With one ventral cirral row	Several separated ventral rows
22	Frontal cirri clearly differentiated	Not distinctly differentiated
23	Caudal cirri present	Absent

over their precise systematic position (Corliss, 1979; Jankowski, 1979; Small & Lynn, 1985; Tuffrau, 1986; de Puytorac *et al.*, 1993; Lynn & Small, 2000).

With reference to their morphology, discocephalines are conspicuously more similar to stichotrichs than to euplotids as follows: both left and right marginal rows are present (cf. only left marginal row present or neither of them present in euplotids); the body is flexible (cf. almost always rigid in euplotids); as in the lower stichotrichs, more than five transverse cirri are present (cf. invariably five in all typical euplotids); they have a relatively small buccal field, with *Oxytricha*-like undulating membranes [cf. generally having a conspicuously large buccal field with (mostly) a single undulating membrane in euplotids]; they possess many macronuclear nodules that are distributed sparsely throughout the cell (cf. usually one macronucleus or, if more than one, macronuclear nodules are closely aligned in euplotids).

Hitherto, morphogenesis has been described for only two discocephalines, *Discocephalus ehrenbergi* Dragesco, 1960 and *Marginotricha faurei* (Dragesco, 1963) Lin *et al.*, 2004 (Dragesco, 1960; Lin *et al.*, 2004). These, along with *P. borrori,* share several morphogenetic features of cortical development including: (i) stomatogenesis is of the epi-apokinetal type; (ii) the caudal cirri derive from the rightmost DK anlagen, which are usually close to the right marginal fragment; (3) DK anlagen appear intrakinetally (secondary mode); (4) there are always more than five (number variable) FVT-anlagen that are formed in the primary mode; (5) the old AZM is either completely retained (e.g. *D. ehrenbergi*) or partly retained with the posterior portion renewed (e.g. *M. faurei* and *P. borrori*), but no new OP is generated (Wicklow, 1982; Foissner, 1996; Berger, 1999, 2006; Song, 2004).

The morphogenetic data reveal that the discocephalines have both stichotrich and hypotrich characteristics (Table 1). Five morphogenetic characters are highly characteristic of the stichotrichs: (i) the OP in the opisthe is generated *de novo* on the cell surface (epi-apokinetal mode); (ii) the two marginal rows are formed intrakinetally, which is typical for most stichotrichs; (iii) more than five FVT-cirral anlagen are formed, a plesiomorphic feature that is shared by the 'lower' stichotrichs; (iv) the new UM in the proter come from dedifferentiated old structures; (v) the dorsal anlagen are formed as two groups (i.e. secondary mode), one anterior and one posterior of the equatorial region. In contrast, there are only two morphogenetic features that are shared by discocephalines and euplotids to the exclusion of stichotrichs: (i) several caudal cirri are formed from the rightmost DK anlagen; (ii) the development of the FVT-anlagen is of the primary type, although this feature also occurs in some lower stichotrichs (Song *et al.*, 1997; Song, 2004). On balance, therefore, the morphogenetic data suggest that the discocephalines are more closely related to the stichotrichs than to the hypotrichs.

Based on the molecular data derived from the complete SSU rDNA sequences, the discocephalines could be ancestral to the stichotrichs and other non-euplotid spirotrich lineages (Fig. 6). This is partly supported by the phylogenetic analyses using morphogenetic information, which suggests that Discocephalina might be an isolated stichotrich clade (Fig. 7).

Clearly, there are discrepancies in the position of discocephalines in the phylogenetic tress derived from morphological/morphogenetic data and molecular data (Figs 6 and 7) and, without doubt, both trees would benefit from an increase in the number of taxa included. In the meantime, and in the absence of any further data, we suggest that the discocephalines should have the taxonomic rank of order (i.e. Discocephalida Wicklow, 1982), as suggested by de Puytorac *et al.* (1993), within the subclass Stichotrichia.

ACKNOWLEDGEMENTS

REFERENCES

Berger, H. (1999). *Monograph of the Oxytrichidae (Ciliophora, Hypotrichia)* (Monographiae Biologicae vol. 78). Dordrecht: Springer.

Berger, H. (2006). *Monograph of the Urostyloidea (Ciliophora, Hypotricha)* (Monographiae Biologicae vol. 85). Heidelberg: Springer.

Corliss, J. O. (1979). *The Ciliated Protozoa: Characterization, Classification and Guide to the Literature*, 2nd edn. New York: Pergamon.

Curds, C. R. & Wu, I. C. H. (1983). A review of the Euplotidae (Hypotrichida, Ciliophora). *Bull Br Mus Nat Hist (Zool)* **44**, 191–247.

de Puytorac, P., Batisse, A., Deroux, G., Fleury, A., Grain, J., Laval-Peuto, M. & Tuffrau, M. (1993). Proposition d'une nouvelle classification du phylum des protozoaires Ciliophora Doflein, 1901. *C R Acad Sci Paris* **316**, 716–720 (in French).

Dragesco, J. (1960). Ciliés mésopsammiques littoraux. Systématique, morphologie, écologie. *Trav Stn Biol Roscoff (N S)* **12**, 1–356 (in French).

Dragesco, J. (1965). Ciliés mésopsammiques d'Afrique noire. *Cah Biol Mar* **6**, 357–399 (in French).

Eigner, P. & Foissner, W. (1994). Divisional morphogenesis in *Amphisiellides illuvialis* n. sp., *Paramphisiella caudata* (Hemberger) and *Hemiamphisiella terricola* Foissner and redefinition of the Amphisiellidae (Ciliophora, Hypotrichida). *J Eukaryot Microbiol* **41**, 243–261.

Foissner, W. (1996). Ontogenesis in ciliated protozoa, with emphasis on stomatogenesis. In *Ciliates, Cells as Organisms*, pp. 95–177. Edited by K. Hausmann & P. C. Bradbury. Stuttgart: Gustav Fischer.

Hu, X. & Song, W. (2001). Morphology and morphogenesis of *Holosticha heterofoissneri* nov. spec. from the Yellow Sea, China (Ciliophora, Hypotrichida). *Hydrobiologia* **448**, 171–179.

Jankowski, A. W. (1979). Revision of the order Hypotrichida Stein, 1859. Generic catalogue, phylogeny, taxonomy. *Akad Nauk SSSR Zool Inst Trudy* **86**, 46–85 (in Russian).

Jerka-Dziadosz, M. & Wiernicka, L. (1992). Ultrastructural studies on the development of cortical structures in the ciliary pattern mutans of the hypotrich ciliate *Paraurostyla weissei*. *Eur J Protistol* **28**, 258–272.

Kumar, S., Tamura, K. & Nei, M. (2004). MEGA3: integrated software for molecular evolutionary genetics analysis and sequence alignment. *Brief Bioinform* **5**, 150–163.

Li, L. & Song, W. (2006). Phylogenetic position of the marine ciliate, *Certesia quadrinucleata* (Ciliophora; Hypotrichida) inferred from the complete small subunit ribosomal RNA gene sequence. *Eur J Protistol* **42**, 55–61.

Lin, X., Song, W. & Warren, A. (2004). Redescription of the rare marine ciliate, *Prodiscocephalus borrori* (Wicklow, 1982) from shrimp-culturing waters near Qingdao, China, with redefinitions of the genera *Discocephalus*, *Prodiscocephalus* and *Marginotricha* (Ciliophora, Hypotrichida, Discocephalidae). *Eur J Protistol* **40**, 137–146.

Lynn, D. H. & Small, E. B. (2000). Phylum Ciliophora Doflein, 1901. In *An Illustrated Guide to the Protozoa*, 2nd edn, pp. 371–656. Edited by J. J. Lee, G. F. Leedale & P. Bradbury. Lawrence, KS: Society of Protozoologists and Allen Press.

Nixon, K. C. (1999). The Parsimony Ratchet, a new method for rapid parsimony analysis. *Cladistics* **15**, 407–414.

Nylander, J. (2004). MrModeltest v. 2. Uppsala: Evolutionary Biology Centre, Uppsala University.

Posada, D. & Crandall, K. A. (1998). Modeltest: testing the model of DNA substitution. *Bioinformatics* **14**, 817–818.

Ronquist, F. & Huelsenbeck, J. P. (2003). MrBayes 3: Bayesian phylogenetic inference under mixed models. *Bioinformatics* **19**, 1572–1574.

Schlegel, M., Elwood, H. J. & Sogin, M. L. (1991). Molecular evolution in hypotrichous ciliates: sequence of the small subunit RNA genes from *Onychodromus quadricornutus* and *Oxytricha granulifera* (Oxytrichidae, Hypotrichida, Ciliophora). *J Mol Evol* **32**, 64–69.

Shao, C., Song, W., Warren, A., Al-Rasheid, K., Yi, Z. & Jun, G. (2006). Morphogenesis of the marine ciliate, *Pseudoamphisiella alveolata* (Kahl, 1932) Song & Warren, 2000 (Ciliophora, Stichotrichia, Urostylida) during binary fission. *J Eukaryot Microbiol* **53**, 388–396.

Shao, C., Song, W., Yi, Z., Gong, J., Li, J. & Lin, X. (2007). Morphogenesis of the marine spirotrichous ciliate, *Trachelostyla pediculiformis* (Cohn, 1866) Borror, 1972 (Ciliophora, Stichotrichia), with consideration of its phylogenetic position. *Eur J Protistol* **43**, 255–264.

Sikes, D. S. & Lewis, P. O. (2001). PAUPRat: PAUP implementation of the parsimony ratchet. Beta software, version 1. Storrs, CT: Department of Ecology and Evolutionary Biology, University of Connecticut.

Small, E. B. & Lynn, D. H. (1985). Phylum Ciliophora Doflein, 1901. In *An illustrated Guide to the Protozoa. Society of Protozoologists*,

pp. 393–575. Edited by J. J. Lee, S. H. Hutner & E. C. Bovee. Lawrence, KS: Allen Press.

Sogin, M. L. & Elwood, H. J. (1986). Primary structure of the *Paramecium tetraurelia* small-subunit rRNA coding region: phylogenetic relationships within the Ciliophora. *J Mol Evol* **23**, 53–60.

Song, W. (1990). A comparative analysis of the morphology and morphogenesis of *Gonostomum strenua* (Engelmann, 1862) (Ciliophora, Hypotrichida) and related species. *J Eukaryot Microbiol* **37**, 249–257.

Song, W. (2001). Morphology and morphogenesis of the marine ciliate, *Ponturostyla enigmatica* (Dragesco & Dragesco-Kernéis) Jankowski, 1989 (Ciliophora, Hypotrichida, Oxytrichidae). *Eur J Protistol* **37**, 181–197.

Song, W. (2004). On cell development of ciliated protozoa: diversity and progress. *J Ocean Univ China* **34**, 747–757 (in Chinese with English summary).

Song, W. & Packroff, G. (1993). Beitrag zur Morphogenese des marinen Ciliaten *Diophrys scutum* (Dujardin, 1841) (Ciliophora, Hypotrichida). *Zool Jahrb Anat* **123**, 85–95 (in German).

Song, W., Warren, A. & Hu, X. (1997). Morphology and morphogenesis of *Pseudoamphisiella lacazei* (Maupas, 1883) Song, 1996 with suggestion of establishment of a new family Pseudoamphisiellidae nov. fam. (Ciliophora, Hypotrichida). *Arch Protistenkd* **147**, 265–276.

Song, W., Wilbert, N., Chen, Z. & Shi, X. (2004). Considerations on the systematic position of *Uronychia* and related euplotids based on the data of ontogeny and 18S rRNA gene sequence analyses, with morphogenetic redescription of *Uronychia setigera* Calkins, 1902 (Ciliophora, Euplotida). *Acta Protozool* **43**, 313–328.

Swofford, D. L. (2002). PAUP*: Phylogenetic analysis using parsimony (and other methods), version 4. Sunderland, MA: Sinauer Associates.

Thompson, J. D., Higgins, D. G. & Gibson, T. J. (1994). CLUSTAL W: improving the sensitivity of progressive multiple sequence alignment through sequence weighting, position-specific gap penalties and weight matrix choice. *Nucleic Acids Res* **22**, 4673–4680.

Tuffrau, M. (1986). Proposition d'une classification nouvelle de l'Ordre Hypotrichida (Protozoa, Ciliophora), fondée sur quelques données récentes. *Ann Sci Nat* **8**, 111–117 (in French).

Tuffrau, M. & Fleury, A. (1994). Classe des Hypotrichea Stein, 1859. *Trop Zool* **2**, 83–151 (in French).

Vos, R. A. (2003). Accelerated likelihood surface exploration: the likelihood ratchet. *Syst Biol* **52**, 368–373.

Wicklow, B. J. (1982). The Discocephalina (n. subord.): ultrastructure, morphogenesis and evolutionary implications of a group of endemic interstitial hypotrichs (Ciliophora, Protozoa). *Protistologica* **18**, 299–330.

Wilbert, N. (1975). Eine verbesserte Technik der Protargolimprägnation für Ciliaten. *Mikrokosmos* **64**, 171–179 (in German).